Fully quantum algorithm for lattice Boltzmann methods with application to partial differential equations

Fatima Ezahra Chrit,[1,2] Sriharsha Kocherla,[2] Bryan Gard,[3]
Eugene F. Dumitrescu,[4] Alexander Alexeev,[1] and Spencer H. Bryngelson[2]

[1] *George W. Woodruff School of Mechanical Engineering, Georgia Institute of Technology, Atlanta, GA 30332, USA*

[2] *School of Computational Science & Engineering, Georgia Institute of Technology, Atlanta, GA 30332, USA*

[3] *CIPHER, Georgia Tech Research Institute, Atlanta, GA 30332, USA*

[4] *Oak Ridge National Laboratory, Oak Ridge, Tennessee 37831, USA*

(Dated: May 15, 2023)

Fluid flow simulations marshal our most powerful computational resources. In many cases, even this is not enough. Quantum computers provide an opportunity to speedup traditional algorithms for flow simulations. We show that lattice-based mesoscale numerical methods can be executed as efficient quantum algorithms due to their statistical features. This approach revises a quantum algorithm for lattice gas automata to eliminate classical computations and measurements at every time step. For this, the algorithm approximates the qubit relative phases and subtracts them at the end of each time step, removing a need for repeated measurements and state preparation (encoding). Phases are evaluated using the iterative phase estimation algorithm and subtracted using single-qubit rotation phase gates. This method delays the need for measurement to the end of the computation, so the algorithm is better suited for modern quantum hardware. We also demonstrate how the checker-board deficiency that the D1Q2 scheme presents can be resolved using the D1Q3 scheme. The algorithm is validated by simulating two canonical PDEs: the diffusion and Burgers' equations on different quantum simulators. We find good agreement between quantum simulations and classical solutions of the presented algorithm.

I. INTRODUCTION

Solving partial differential equations (PDEs) is necessary for modeling most scientific problems. However, it is computationally expensive, especially for large domains and high-dimensional configuration spaces. For example, in computational fluid dynamics, the cost of performing a direct numerical simulation of turbulence increases with Reynolds number, representing the ratio of inertial to viscous effects in the flow, as $\mathcal{O}(\mathrm{Re}^3)$ [1]. Such high computational expense motivates a broad category of work on achieving algorithmic speedups for PDE solvers.

Quantum computers are emerging as an increasingly viable tool for algorithm speedup enabled by the principles of quantum mechanics, such as superposition and entanglement. In some cases, exponential speedups over classical computer architectures (like that of von Neumann) are possible [2, 3]. In the sciences, algorithmic complexity improvements are seen in quantum chemistry [4], machine learning [5–7], finance [8, 9], and more.

Quantum algorithms for solving PDEs have also gained attention. Harrow *et al.* [10] demonstrated the first quantum algorithm, HHL, for solving linear systems of equations with exponential speedup. Such improvements can be marshaled in the PDE space for solving discretized systems of equations via, for example, the method of lines. Childs and Liu [11] proposed a quantum algorithm for linear ordinary differential equations (ODEs) based on spectral methods, providing a global approximation to the solution using linear combinations of basis functions. Childs *et al.* [12] improved the complexity of quantum algorithms for linear PDEs using adaptive-order finite difference and spectral methods. Other

Corresponding author: shb@gatech.edu

approaches to solving PDEs were proposed by Berry [13]; for example, reducing an ODE system via discretization and solving it via the appropriate quantum algorithms. Gaitan [14] used this approach to solve the 1D Navier–Stokes equations for the flow through a convergent-divergent nozzle. However, these methods require deep circuits and many quantum gates to achieve results comparable to what one can solve on even a modern laptop. This proves prohibitive for most of the above-mentioned algorithms but paints a bright future for larger, fault-tolerant quantum devices that can better reject gate noise.

In the near term, variational quantum algorithms are well-suited for current NISQ (noisy intermediate-scale quantum) devices. For example, hybrid quantum–classical procedures can evaluate the solution quality via a cost function using a quantum computer and optimize variational parameters using a classical computer. Thus, variations methods enable quantum algorithms with relatively shallow gate depths and qubit counts. Bravo-Prieto *et al.* [15] introduced the variational quantum linear solver (VQLS), which uses the Hadamard test to solve a linear system. Liu *et al.* [16] showed that a Poisson problem can be solved by first converting it to a linear system amenable to the Quantum Alternating Operator Ansatz (QAOA) algorithm. However, variation algorithms require a (sometimes) unclear ansatz and do not guarantee convergence or speedup. The continued tension between these quantum algorithm threads has contributed to improving each.

Because of the linearity of quantum mechanics, quantum algorithms aiming to solve nonlinear PDEs are immature compared to the linear case. Liu *et al.* [17] proposed the first quantum algorithm for dissipative nonlinear differential equations using the method of Carleman linearization, which maps the system of nonlinear equations to an infinite-dimensional system of linear differential equations, which are then solved using quantum linear system algorithms. Their algorithm was tested to solve the 1D Burgers' equation. Kyriienko *et al.* [18] used the variational method based on differentiable quantum circuits to solve nonlinear differential equations. Their method solved a quasi-1D approximation of Navier–Stokes equations. Lubasch *et al.* [19] used multiple copies of variational quantum states and tensor networks to solve nonlinear PDEs.

Other promising numerical methods include mesoscale methods, which operate between molecular and continuum scales. Lattice methods are a common example and are well suited for quantum computation because they are intrinsically statistical, resolving only samples or probabilities of the fictitious particles they comprise. Moreover, they are based on simple mathematical calculations and are suitable for parallel computation because interactions between lattice nodes are linear, and non-linearity enters during a local collision step. The lattice Boltzmann method (LBM) is a common such approach that solves the Boltzmann transport equation. Mezzacapo *et al.* [20] developed the first quantum simulator following a lattice kinetic formalism to solve fluid dynamics transport phenomena. Todorova and Steijl [21] solved the collisionless Boltzmann equation on a quantum computer, inspired by quantum algorithms solving the Dirac equation. Budinski [22] proposed a novel quantum algorithm that solves the advection–diffusion equation by the LBM and extended it to solve the 2D Navier–Stokes equations using stream function–vorticity formulation [23]. Itani and Succi [24] explored the Carleman linearization of the collision term of the lattice Boltzmann equation. Using this linearization technique, Itani *et al.* [25] proposed a quantum lattice Boltzmann algorithm where collision and streaming are both achieved by unitary evolution.

The LBM originates from the lattice gas automata (LGA), a cellular automaton that can simulate fluid flows. A quantum computer can be viewed as a quantum cellular automaton (QCA), where each cell is a quantum system with a state depending on neighboring cells. Quantum LGA is a subclass of QCA that represents particles interacting under physical constraints and evolving on a lattice. The main drawback of the LGA is statistical noise, though this vanishes when crafted for mesoscopic scales. Yepez [26] introduced the first quantum LGA (QLGA) algorithm for simulating fluid flow at the mesoscopic scale using a discretized Boltzmann transport equation. This algorithm was designed for a specialized Type-II quantum computer, proposed in the early 2000s [27]. Such computers consisted of several small quantum computers connected by classical communication channels, allowing qubit shifts during the algorithm's streaming step [27]. The algorithm also requires estimating the distribution functions needed to re-prepare the quantum states at each time step. Re-preparation entails measuring each qubit at the end of each time step, a process that substantially increases computational time on current superconducting quantum computers.

Herein, we present an approach that overcomes the limitations of previous lattice-based quantum algorithms and is more suitable for modern quantum hardware. The algorithm uses a quantum implementation of the streaming step, approximates the qubit relative phases, and subtracts them at the end of each time step, avoiding repeated encoding operations and delaying the need for measurement to the end of the computation. Validation is achieved via

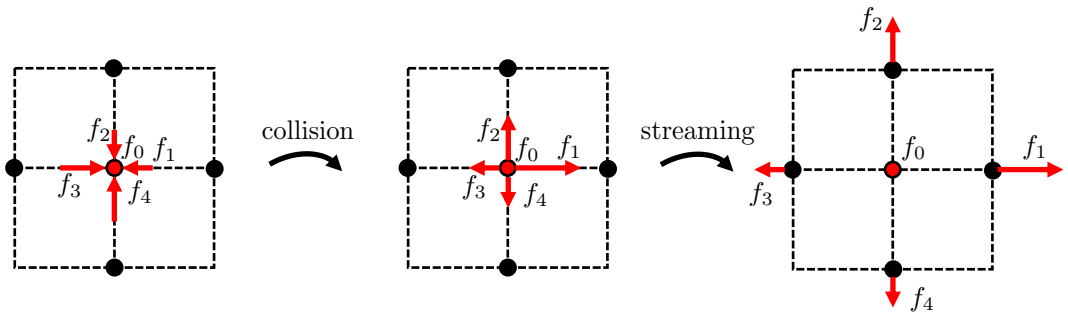

FIG. 1. Illustration of the two main LBM operations: collision and streaming.

implementation in Qiskit [28] and tested the diffusion and Burgers' equations.

This manuscript continues as follows. Section II describes the classical lattice gas automata and lattice Boltzmann method. Section III introduces the quantum counterpart of the classical LGA. Section IV presents the QLGA variants we propose, including quantum streaming, the D1Q3 scheme, and a measurement-avoiding algorithm. We validate these variants by testing them to solve the 1D diffusion and Burgers' equations. Last, section V compares different quantum simulation strategies for the proposed algorithm using Qiskit and XACC.

II. CLASSICAL LATTICE GAS

The lattice gas automata (LGA) method is a cellular automaton used to simulate fluids [29, 30]. The LGA state is described by *occupation numbers*: Boolean variables indicating whether or not a fictitious particle is present at a specific lattice node, moving in a certain lattice direction at a specific time. These fictitious particles obey local collision rules that conserve mass and momentum.

The main drawback of LGA is noise, which can be reduced by coarse-graining over large domains or time intervals, but remains costly in computing time and memory. Instead, the LGA can be directly modeled at the mesoscopic scale with the Boltzmann equation [31, 32]. This approach is called the lattice Boltzmann method (LBM), which eliminates the LGA noise by replacing Boolean variables with continuous distributions, i.e., the mean occupation numbers, also called density distribution functions. The LBM approach replaces the collision rule with a continuous function called the collision operator. The distribution functions f_α $(0 \leq f_\alpha \leq 1)$ evolve in time according to the kinetic equation

$$f_\alpha(\boldsymbol{r} + \boldsymbol{c}_\alpha \Delta t, t + \Delta t) = f_\alpha(\boldsymbol{r}, t) + \Omega_\alpha[f_\alpha(\boldsymbol{r}, t)], \tag{1}$$

where $\boldsymbol{r}$ is the position of a lattice site, $\boldsymbol{c}_\alpha$ is the lattice velocity, Δt is the time step, t is time, Ω_α is the collision operator, and α refers to the velocity discretization index. During one time step, the computation evolves through two processes: collision, where particles meet at the same lattice site and their distribution functions are evaluated according to the collision operator Ω_α, and streaming, where particles shift to the neighboring sites following their lattice directions. Collision causes the relaxation of all local distribution functions to an equilibrium where $\Omega_\alpha[f_\alpha = f_\alpha^{\text{eq}}] = 0$.

Each discretization of the velocity space is described by its number of spatial dimensions a and velocity directions b, with scheme notation DaQb. For example, a D1Q2 scheme uses a 1D lattice with two velocity directions, i.e., a right-going particle and a left-going particle for each lattice site.

Macroscopic variables, like the fluid density or velocity, are determined from the moments of the distribution functions [33]. For example, the density at lattice site i corresponds to

$$\rho_i = \sum_{\alpha=1}^{b} f_{\alpha,i}. \tag{2}$$

Herein, we divide 1D spatial domains into N_s uniformly spaced lattice sites $i = 0, \ldots, N_s - 1$. For example, domain

$X \in [0, L]$ has site locations $x_i = i\Delta x$ where $\Delta x = L/N_s$ is the lattice spacing, usually set to 1.

III. QUANTUM LATTICE GAS

The quantum LGA (QLGA) is a measurement-based algorithm that introduces a superposition of qubit states within a small spatial region and for a short period. It directly maps the bits used in a classical lattice gas to qubits and models the lattice gas at the mesoscopic scale, which can be described using the lattice Boltzmann equation. Figure 2 shows an example of the associated quantum circuit used to solve the 1D diffusion equation using the D1Q2 scheme defined in the previous section. The algorithm has four operations: (re)initializing the qubit states via *encoding*, *collision* at each lattice site, measuring the qubit occupancy via *localization*, and *streaming* the qubits on the lattice appropriately. Encoding and collision are performed in the quantum space, but the measurement step and classical streaming computation mean the quantum state must be re-encoded.

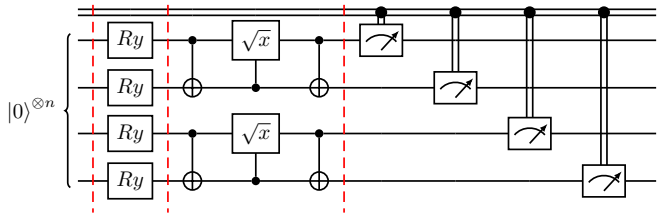

FIG. 2. QLGA with classical streaming [26]. R_y is a rotation gate by the angle $\theta_\alpha = 2\arccos\sqrt{1 - f_\alpha(x_i, t)}$ for the qubit of state $|q_\alpha(x_i, t)\rangle$. The controlled $\sqrt{x}$ gate is a native IBM gate, decomposed as a two-qubit controlled phase rotation $P(\pi/2)$ gate between two Hadamard gates on the target qubit [34].

The system wavefunction can be written as

$$|\Psi(x_0, x_1, \ldots, x_{N_s-1}, t)\rangle = \bigotimes_{i=0}^{N_s-1} |\Psi(x_i, t)\rangle \,. \tag{3}$$

Following Dirac's bra-ket notation, the ket vector $|\Psi(x_i, t)\rangle$ represents the on-site state, i.e., at the lattice site of coordinate x_i, of dimension 2^b. In the D1Q2 scheme, each lattice site comprises two particles, one moving to the right and the other to the left. QLGA maps the two particles to qubits, denoted by $|q_\alpha(x_i, t)\rangle$ where $\alpha = 1, 2$. The α-th qubit encodes an occupancy probability $f_\alpha(x_i, t)$ at lattice site x_i and time t.

In the first step of the QLGA algorithm, qubits encode the occupancy probabilities via this expression:

$$|q_\alpha(x_i, t)\rangle = \sqrt{1 - f_\alpha(x_i, t)}\,|0\rangle + \sqrt{f_\alpha(x_i, t)}\,|1\rangle \quad \text{for} \quad i = 0, \ldots, N_s - 1 \quad \text{and} \quad \alpha = 1, 2. \tag{4}$$

The on-site ket vector representing the quantum state at each lattice site x_i is

$$|\Psi(x_i, t)\rangle = |q_1(x_i, t)\rangle \otimes |q_2(x_i, t)\rangle \quad \text{for} \quad i = 0, \ldots, N_s - 1. \tag{5}$$

This step is implemented via the $R_y(\theta_\alpha)$ rotation gate by the angle $\theta_\alpha = 2\arccos\sqrt{1 - f_\alpha(x_i, t)}$ for the qubit of state $|q_\alpha(x_i, t)\rangle$. The relative phase of the qubits is set to zero in this step. Then, QLGA applies the collision locally to each lattice site, a unitary operation that relaxes the distribution functions to equilibrium. The post-collision state is

$$|\Psi'(x_i, t)\rangle = U\,|\Psi(x_i, t)\rangle \tag{6}$$

where U is the collision operator that causes local quantum entanglement of the on-site qubits. It is implemented via a

unitary gate with a block-diagonal entangling $U(2)$ matrix:

$$\begin{pmatrix} 1 & 0 & 0 & 0 \\ 0 & e^{i\phi}e^{i\xi}\cos\theta & e^{i\phi}e^{i\zeta}\sin\theta & 0 \\ 0 & -e^{i\phi}e^{-i\zeta}\sin\theta & e^{i\phi}e^{-i\xi}\cos\theta & 0 \\ 0 & 0 & 0 & 1 \end{pmatrix} \tag{7}$$

where ϕ, ξ, ζ, and θ are Euler angles chosen to satisfy the PDE of interest in the continuum limit. We choose $\phi = -\pi/4$, $\xi = 0$, $\zeta = \pi/2$ and $\theta = \pi/4$ to model the diffusion equation and $\phi = 0$, $\xi = \zeta$ and $\theta = \pi/4$ to model Burgers' equation [35, 36].

Next, all qubits are measured, and the post-collision occupancy probabilities $f'_\alpha(x_i, t)$ are computed from measurement outcomes. The non-unitary measurement operation destroys the quantum superposition and entanglement that the collision step may have caused. The post-collision occupancy probability is

$$f'_\alpha(x_i, t) = \langle \Psi'(x_i, t)| \, n_\alpha \, |\Psi'(x_i, t)\rangle \tag{8}$$

where n_α are the number operators for $\alpha = 1, 2$.

Then, streaming is performed by shifting the qubits to their neighboring positions according to their right or left lattice directions. The post-streaming occupancy probabilities can be written as

$$f_\alpha(x_i, t + \Delta t) = f'_\alpha(x_i + e_\alpha \Delta x, t), \tag{9}$$

where $e_1 = -1$ and $e_2 = 1$ are the qubits directions, Δx is the spacing, and Δt is the time step.

These four operations can be encapsulated in the following equation:

$$f_\alpha(x_i + e_\alpha \Delta x, t + \Delta t) = f_\alpha(x_i, t) + \Omega_\alpha[f_\alpha(x_i, t)] \tag{10}$$

which is in the form of the classical lattice Boltzmann equation with the collision operator given by:

$$\Omega_\alpha[f_\alpha(x_i, t)] = \langle \Psi(x_i, t)| \, U^\dagger n_\alpha U - n_\alpha \, |\Psi(x_i, t)\rangle \tag{11}$$

Equilibrium distributions can be found by satisfying the equilibrium condition: $\Omega_\alpha[f_\alpha = f_\alpha^{\text{eq}}] = 0$. For the diffusion equation, we get equal equilibrium probabilities $f_\alpha^{\text{eq}} = \rho/2$ for $\alpha = 1, 2$. For Burgers' equation, the equilibrium distribution corresponds to $f_\alpha^{\text{eq}} = \rho/2 + e_\alpha/2(\sqrt{2} - \sqrt{1 + (\rho - 1)^2})$.

This streaming step was designed to run classically on Type-II quantum computers [27]. One time step of QLGA consists of the four operations described above. Unlike most quantum gate models, where measurement is performed at the end of the computation, QLGA requires measurement at each time step to extract the distribution functions, which are then used to encode the next time step. The recurrent decoherence at each lattice site is necessary to allow qubits to shift to neighboring sites classically. We next present a method for avoiding these unnecessary computations on modern quantum hardware.

IV. A FULLY-QUANTUM LATTICE BOLTZMANN ALGORITHM

This section presents a single-quantum computer version of QLGA that avoids the Type-II quantum computers of previous studies. We formulate a fully-quantum lattice Boltzmann method algorithm (QLBM) and verify it against known, classical solutions. Since the QLGA solves the lattice Boltzmann equation at the mesoscopic scale, we shall name our QLGA variants as QLBM.

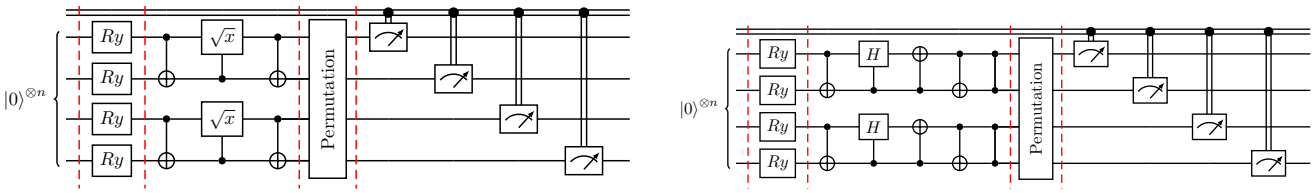

(a) QLBM circuit solving the diffusion equation

(b) QLBM circuit solving Burgers' equation

FIG. 3. QLBM with quantum streaming solving (a) the diffusion equation and (b) Burgers' equation. The permutation block encapsulates a sequence of swap gates that shift the qubits during the streaming step.

A. Quantum streaming

The first revision to the QLGA algorithm performs the streaming step using quantum states, not classically. It can be implemented before the measurement step via the permutation function that applies a sequence of swap gates to shift the qubits to their neighbors. The corresponding quantum circuit is shown in fig. 3 for the diffusion and Burgers' equations.

We validate the proposed variant by solving the 1D diffusion equation and Burgers' equation using Gaussian and sinusoidal distributions as the initial condition, respectively. Periodic boundary conditions are used. We compare the two QLBM solutions, i.e., with classical streaming and quantum streaming, with the classical solution using the D1Q2 scheme and 26 simulated qubits. The simulations were performed using Qiskit AerSimulator with the statevector simulation method, and the counts were sampled from the statevector using 10^5 shots. The spatial domain consists of $N_s = 13$ lattice sites corresponding to 26 qubits. Results are shown after 10 time steps.

The results of fig. 4 demonstrate good agreement with the classical solution. This variant removes the need for classical communication between lattice sites and does not cause global entanglement, as swap gates merely interchange the qubit quantum states.

In terms of complexity, we examine the relationship between the circuit depth and the system size by analyzing the different operations of the algorithm separately. The encoding step consists of applying one rotation gate simultaneously to each qubit. Thus, changing the grid resolution and the qubit number does not affect the circuit depth. The same unitary operator is applied to each pair of qubits for the collision step. Thus, the circuit depth scales as $\mathcal{O}(1)$ with the number of qubits n. For the streaming step implemented using the permutation function, the number of swap gates applied to one of the qubits increases linearly with the number of qubits. Therefore, the complexity of the algorithm is given by $\mathcal{O}(n)$.

B. 1-dimension, three-velocities: D1Q3 scheme

The implementations of the QLBM mentioned above used the D1Q2 scheme, which uses two moving particles per lattice site. This scheme shows checker-board pathologies when using a sharp function as the initial condition because it simulates two independent sub-lattice [26]. Yepez [35] presents a cure for this, allowing only one qubit to move while the other remains stationary. However, this requires two collision and streaming procedures per time step. We show that a quantum D1Q3 scheme, which adds a stationary qubit to each lattice site, solves this problem. A similar solution was demonstrated on three-qubit Type-II quantum computers by Scoville [37].

Figure 5 compares the quantum solution of the diffusion equation using the D1Q2 scheme with the D1Q3 scheme for a delta function as the initial condition. These simulations were performed using the Qiskit matrix product state simulator, 45 qubits for the D1Q3 scheme, and the sampling procedure used 10^6 shots. The spatial domain consists of $N_s = 15$ lattice sites, and results are shown after 10 time steps. The result shows the agreement of the quantum D1Q3 solution with the classical one and how the D1Q3 version remedies the checker-board effect. We note that the D1Q3 scheme does not affect algorithm complexity.

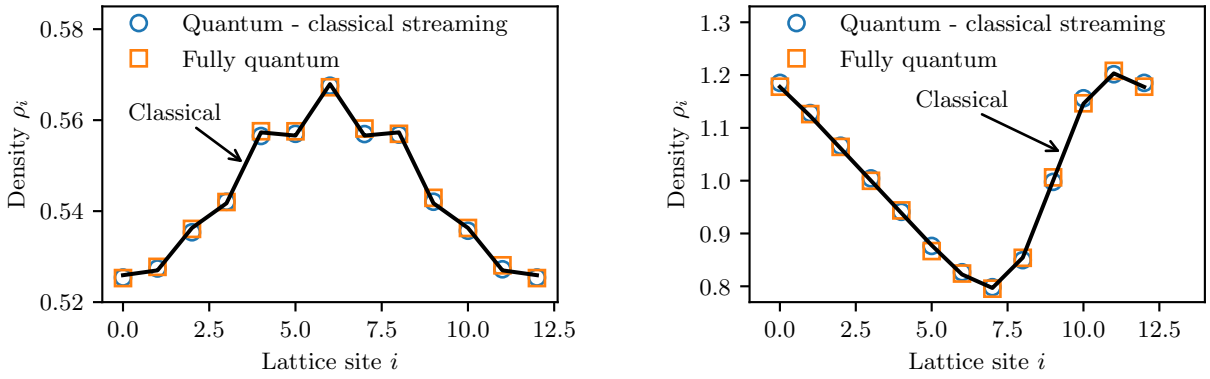

(a) Diffusion equation

(b) Burgers' equation

FIG. 4. QLBM solutions to the diffusion equation (a) and Burgers' equation (b) using the D1Q2 scheme. "Quantum - classical streaming" is associated with the classical streaming algorithm discussed in previous work [26],"Fully quantum" refers to the present algorithm, and "Classical" is the classical implementation of the lattice method.

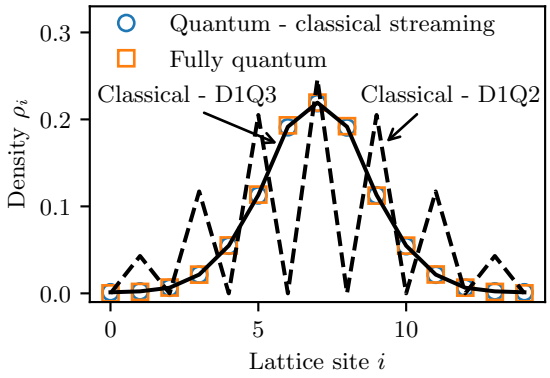

FIG. 5. QLBM solutions to the diffusion equation using the D1Q3 scheme. "Quantum - classical streaming" is associated with the classical streaming algorithm discussed in previous work [26], "Fully quantum" refers to the present algorithm, and "Classical" is the classical implementation of the lattice methods as labeled.

C. Measurement-avoiding QLBM

The quantum state collapses due to measurements performed during each time step, requiring re-encoding. However, we should allow the qubits to explore more complex states to achieve truly quantum computation. Furthermore, measurement on superconducting quantum computers can typically take an order of magnitude longer than gate times, adding significant time to the algorithm [38]. Thus, the goal is to eliminate repeated initialization of the quantum state and repeated measurements, which destroy the quantum superposition and entanglement.

We attempted a unitary transformation using random rotations to reset the qubit relative phases after each time step. However, this random phase kicking leads to dephasing, where the expected value of the off-diagonal elements of the density matrix decay to zero with time [39]. Therefore, a different approach is needed.

To this end, our algorithm adds a phase-correction step, approximating the qubit relative phases and subtracting them at the end of each time step, delaying the need for measurement until the end of the computation. This can be achieved by using the quantum phase estimation (QPE) algorithm as a sub-routine to estimate the eigen-phases of the encoding and collision unitaries [39]. These eigen-phases are then used to classically estimate the qubit relative phases, subtracted at the end of each time step. The accuracy of the QPE depends on the number of ancillary qubits it uses. Thus, we use the iterative phase estimation (IPE) algorithm, which only requires a single auxiliary qubit and evaluates

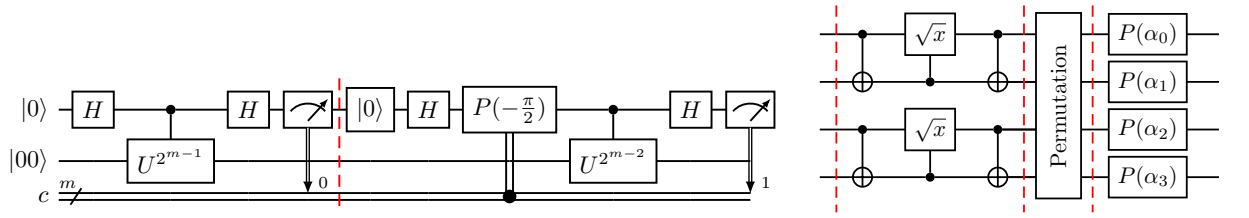

(a) First two iterations of IPE algorithm (b) Measurement-avoiding QLBM circuit

FIG. 6. (a) IPE circuit used to estimate the qubits relative phase α_i and (b) Measurement-avoiding QLBM circuit solving the diffusion equation.

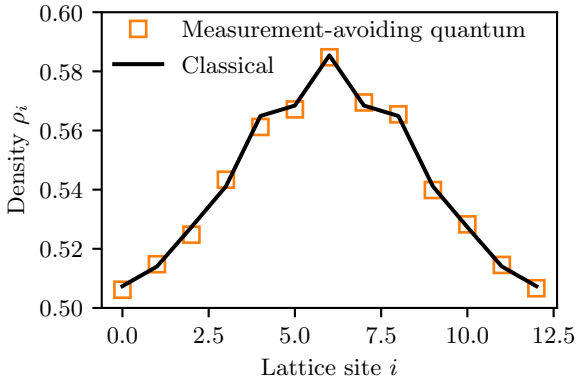

FIG. 7. Measurement-avoiding QLBM (present work) solution to the diffusion equation using the IPE algorithm and its comparison to classical results for the same method and resolution.

the phase bit by bit through a repetitive process [40]. The accuracy of the IPE algorithm is determined by the number of iterations instead of the number of ancillary qubits. Therefore, they are of great importance for near-term quantum computing. The IPE algorithm still requires measurement to estimate the phase. However, only one qubit, i.e. the auxiliary qubit is measured and not all qubits in the quantum register.

In the context of QLBM, we apply the IPE algorithm to every lattice site, i.e., to a two-qubit unitary for the D1Q2 scheme. We set the unitary U to be the product of the encoding and the collision operations since the streaming step only swaps the qubits and does not change their phases. For a total number of iterations m, the IPE algorithm estimates the phase $\varphi = 0.\varphi_1 ... \varphi_m$, where φ_k are the phase bits ($1 \leq k \leq m$). At each iteration k, the IPE algorithm applies the unitary U 2^{m-k} times controlled on the auxiliary qubit. Due to phase kickback, the relative phase of the auxiliary qubit becomes $\exp(i2\pi 0.\varphi_{m-k+1}\varphi_{m-k+2}...\varphi_m)$. Thus, to estimate the phase bit φ_{m-k+1}, a phase correction of $-2\pi(\varphi_{m-k+2}/2^2 + ... + \varphi_m/2^m)$ is performed, controlled on the measurement outcome of the previously estimated phase bits $\varphi_{m-k+2}, ..., \varphi_m$. The phase bit φ_{m-k+1} is then estimated by measuring the auxiliary qubit in the x-basis. The first two iterations of the IPE, which estimates the two least significant bits of the phase φ_m and φ_{m-1}, is illustrated in fig. 6 (a). One time step of the measurement-avoiding QLBM circuit is shown in the circuit of fig. 6 (b), which consists of collision, streaming, and phase correction operations.

Figure 7 presents the numerical simulation of our variant using the IPE algorithm to solve the 1D diffusion equation. The simulation uses the D1Q2 scheme with 26 qubits and runs on the statevector simulator. The spatial domain consists of $N_s = 13$ lattice sites, and results are shown after 6 time steps. A good agreement is found between the quantum solution and the classical one. This variant improves the efficiency of the QLGA algorithm as the encoding is used only once at the beginning of the computation to prepare the quantum states, and measurement is only performed at the end of the computation. However, this algorithm is hybrid since the qubits phases are classically computed from the eigenvalues estimated using the IPE. In terms of complexity, having only one ancillary qubit comes with the cost of $O(2^{m-1})$ gates, where m is the number of IPE iterations related to the precision of the estimated phases.

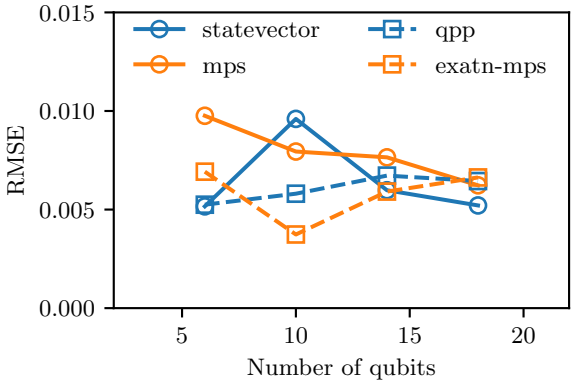

(a) RMSE compared to the classical solution using 10^4 shots

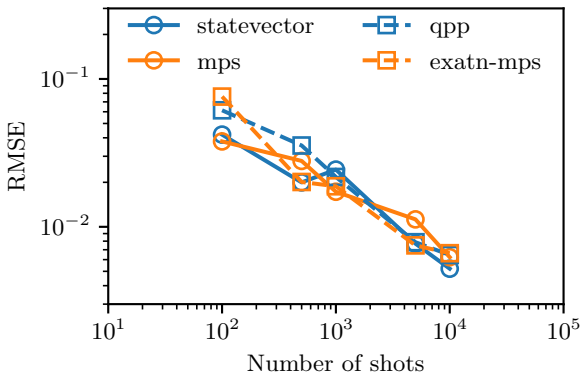

(b) RMSE compared to the classical solution using 18 qubits

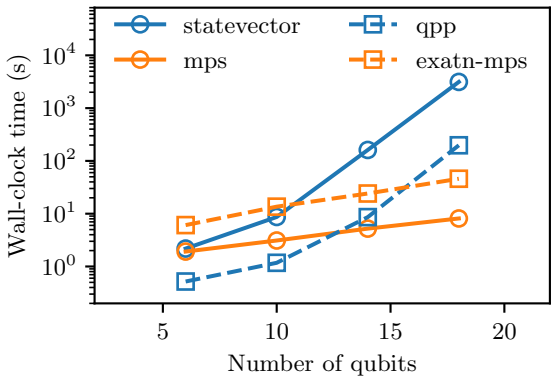

(c) Wall-clock time in seconds using 10^4 shots

FIG. 8. RMSE and wall-clock time of the quantum solution solving the diffusion equation compared to the classical one. Qiskit (solid lines, ——) statevector and mps simulators and XACC simulators (dashed lines, – – –) qpp and exatn-mps are shown. The colors correspond to (blue) statevector-like and (orange) matrix product state simulators.

V. QUANTUM SIMULATORS

We test different quantum simulator implementations of our QLBM algorithm and its circuit. Simulators include statevector-based and tensor-network types that use the matrix product state (mps) method [41]. Two different simulation frameworks are tested: Qiskit and XACC [42]. Statevector and mps simulators are part of the Qiskit Aer backend. The XACC qpp (Quantum++) simulator is based on a C++ general-purpose quantum computing library [43]. XACC exatn-mps simulator is a part of the TNQVM (tensor-network quantum virtual machine) simulation backend and uses a noiseless, matrix product state wave function decomposition for the quantum circuit [44]. The wall-clock times of fig. 8 (c) were obtained via simulation on an AMD EPYC 7742 (64-core) processor.

We run the QLBM circuit of fig. 3 on the four different simulators and compare their performance. Figure 8 shows the wall-clock time and the root-mean-squared error (RMSE),

$$\mathrm{RMSE} = \sqrt{\frac{\sum_{i=0}^{N_s-1}\left(\rho_i^{(\mathrm{quant.})} - \rho_i^{(\mathrm{classic.})}\right)^2}{N_s}}, \tag{12}$$

where N_s is the number of lattice sites of the quantum solution compared to the classical one as a function of the number of shots (samples from the underlying density functions). The errors are reported from simulations using 10^4

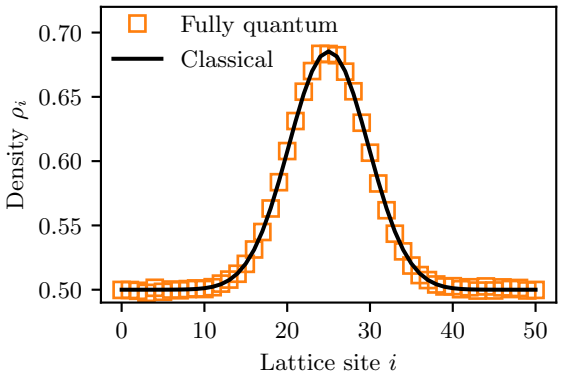

FIG. 9. QLBM solution to the diffusion equation using the Qiskit mps simulator and its comparison to classical results using 102 qubits.

shots in fig. 8 (a) and using 18 qubits in fig. 8 (b). We find that the results are shot-noise limited and all quantum simulators obtain the same accuracy in terms of RMSE, which decreases from less than 10% for 10^2 shots to less than 1% for 10^4 shots. However, the Qiskit mps simulator is at least one order of magnitude faster than the statevector ones. This behavior is expected. The Qiskit statevector and XACC (qpp) simulators generate the full state vector, which scales exponentially with the number of qubits. In contrast, the mps simulator uses a local representation in a factorized form of tensor products [45]. The mps method ensures that the overall structure remains small as long as the circuit has a low degree of entanglement, enabling more simulated qubits. To demonstrate this, we run the QLBM circuit of fig. 3 a on Qiskit mps simulator for the resolution of 51 lattice sites corresponding to 102 qubits using 10^6 shots. Results after 10 time steps are shown in fig. 9 and demonstrate good agreement with the classical solution.

VI. CONCLUSION AND DISCUSSION

In this work, we present a revised quantum lattice gas algorithm that can be used to simulate fluid flows. The algorithm of Yepez [46] was designed for Type-II quantum computers that are no longer used. The presented algorithm uses a full-quantum implementation of the streaming step to eliminate classical communication between lattice sites. In addition, it avoids repetitive measurements and encoding operations by estimating the qubit relative phases and subtracting them at the end of each time step. This eliminates the need for state re-preparation between time steps and delays the need for measurement to the end of the computation. The algorithm is tested to solve canonical PDEs: the diffusion and Burgers' equations. We explored different quantum simulators available on Qiskit and XACC quantum computing frameworks and compare their performance and wall-clock time. Matrix product state simulators are most efficient for the presented quantum circuits, as they have low and local entanglement. These strategic algorithm improvements enable the execution of the quantum lattice gas algorithm on quantum hardware, a subject of future work.

An important limitation of the current algorithm is the size of the required quantum register, which scales linearly with the number of lattice sites. For example, the number of required qubits in a two-dimensional $M \times M$ lattice is $5M^2$ using the D2Q5 scheme. This requirement constrains the ability to extend this algorithm to higher dimensions due to the limited number of qubits available on current quantum hardware. Thus, one needs to use more appropriate encoding schemes, such as one that scales logarithmically with the number of lattice sites, like amplitude-based encoding. For example, Budinski [22] implements the streaming step via a quantum random walk, similar to the collisionless Boltzmann equation solved on a quantum computer of Todorova and Steijl [21]. Indeed, in principle, one could design an algorithm that uses a quantum random walk for both the collision and streaming operations, which we will investigate in future work.

ACKNOWLEDGEMENTS

We thank Dr. Jeffrey Yepez for numerous fruitful discussions of this work. S.H.B. acknowledges support from the Georgia Tech Quantum Alliance and a Georgia Tech Seed Grant. E.F.D. acknowledges DOE ASCR funding under the Quantum Computing Application Teams program, FWP number ERKJ347. This work used Bridges2 at the Pittsburgh Supercomputing Center through allocation PHY210084 from the Advanced Cyberinfrastructure Coordination Ecosystem: Services & Support (ACCESS) program, which is supported by National Science Foundation grants #2138259, #2138286, #2138307, #2137603, and #2138296.

[1] S. B. Pope, *Turbulent flows* (Cambridge University Press, 2000).
[2] L. K. Grover, A fast quantum mechanical algorithm for database search, in *Proceedings of the twenty-eighth annual ACM symposium on Theory of Computing* (1996) pp. 212–219.
[3] P. W. Shor, Algorithms for quantum computation: Discrete logarithms and factoring, in *Proceedings of the 35th Annual Symposium on Foundations of Computer Science* (IEEE, 1994) pp. 124–134.
[4] Y. Cao, J. Romero, J. P. Olson, M. Degroote, P. D. Johnson, M. Kieferová, I. D. Kivlichan, T. Menke, B. Peropadre, N. P. Sawaya, *et al.*, Quantum chemistry in the age of quantum computing, Chemical Reviews **119**, 10856 (2019).
[5] P. Wittek, *Quantum machine learning: What quantum computing means to data mining* (Academic Press, 2014).
[6] M. Schuld, I. Sinayskiy, and F. Petruccione, The quest for a quantum neural network, Quantum Information Processing **13**, 2567 (2014).
[7] F. Marquardt, Machine learning and quantum devices, SciPost Physics Lecture Notes **29** (2021).
[8] D. J. Egger, C. Gambella, J. Marecek, S. McFaddin, M. Mevissen, R. Raymond, A. Simonetto, S. Woerner, and E. Yndurain, Quantum computing for finance: State-of-the-art and future prospects, IEEE Transactions on Quantum Engineering **1**, 1 (2020).
[9] A. Bouland, W. van Dam, H. Joorati, I. Kerenidis, and A. Prakash, Prospects and challenges of quantum finance, arXiv preprint arXiv:2011.06492 (2020).
[10] A. W. Harrow, A. Hassidim, and S. Lloyd, Quantum algorithm for solving linear systems of equations, Physical Review Letters **103**, 150502 (2009).
[11] A. M. Childs and J.-P. Liu, Quantum spectral methods for differential equations, Communications in Mathematical Physics **375**, 1427 (2020).
[12] A. M. Childs, J.-P. Liu, and A. Ostrander, High-precision quantum algorithms for partial differential equations, arXiv preprint arXiv:2002.07868 (2021).
[13] D. W. Berry, High-order quantum algorithm for solving linear differential equations, Journal of Physics A: Mathematical and Theoretical **47**, 105301 (2014).
[14] F. Gaitan, Finding flows of a Navier–Stokes fluid through quantum computing, npj Quantum Information **6**, 61 (2020).
[15] C. Bravo-Prieto, R. LaRose, M. Cerezo, Y. Subasi, L. Cincio, and P. J. Coles, Variational quantum linear solver, arXiv preprint arXiv:1909.05820 (2020).
[16] H.-L. Liu, Y.-S. Wu, L.-C. Wan, S.-J. Pan, S.-J. Qin, F. Gao, and Q.-Y. Wen, Variational quantum algorithm for the Poisson equation, Physical Review A **104**, 022418 (2021).
[17] J.-P. Liu, H. Ø. Kolden, H. K. Krovi, N. F. Loureiro, K. Trivisa, and A. M. Childs, Efficient quantum algorithm for dissipative nonlinear differential equations, Proceedings of the National Academy of Sciences **118**, e2026805118 (2021).
[18] O. Kyriienko, A. E. Paine, and V. E. Elfving, Solving nonlinear differential equations with differentiable quantum circuits, Physical Review A **103**, 052416 (2021).
[19] M. Lubasch, J. Joo, P. Moinier, M. Kiffner, and D. Jaksch, Variational quantum algorithms for nonlinear problems, Physical Review A **101**, 010301 (2020).
[20] A. Mezzacapo, M. Sanz, L. Lamata, I. Egusquiza, S. Succi, and E. Solano, Quantum simulator for transport phenomena in fluid flows, Scientific Reports **5**, 1 (2015).
[21] B. N. Todorova and R. Steijl, Quantum algorithm for the collisionless Boltzmann equation, Journal of Computational Physics **409**, 109347 (2020).
[22] L. Budinski, Quantum algorithm for the advection–diffusion equation simulated with the lattice Boltzmann method, Quantum Information Processing **20**, 57 (2021).
[23] L. Budinski, Quantum algorithm for the Navier–Stokes equations, arXiv preprint arXiv:2103.03804 (2021).
[24] W. Itani and S. Succi, Analysis of carleman linearization of lattice boltzmann, Fluids **7**, 24 (2022).

[25] W. Itani, K. R. Sreenivasan, and S. Succi, Quantum algorithm for lattice boltzmann (qalb) simulation of incompressible fluids with a nonlinear collision term, arXiv preprint arXiv:2304.05915 (2023).

[26] J. Yepez, Quantum lattice-gas model for computational fluid dynamics, Physical Review E **63**, 046702 (2001).

[27] J. Yepez, Type-II quantum computers, International Journal of Modern Physics C **12**, 1273 (2001).

[28] Qiskit Community, Qiskit: An open-source framework for quantum computing (2017).

[29] U. Frisch, D. d'Humières, B. Hasslacher, P. Lallemand, Y. Pomeau, and J.-P. Rivet, Lattice gas hydrodynamics in two and three dimensions, in *Lattice Gas Methods for Partial Differential Equations* (CRC Press, 2019) pp. 77–136.

[30] U. Frisch, B. Hasslacher, and Y. Pomeau, Lattice-gas automata for the Navier–Stokes equation, in *Lattice Gas Methods for Partial Differential Equations* (CRC Press, 2019) pp. 11–18.

[31] G. R. McNamara and G. Zanetti, Use of the Boltzmann equation to simulate lattice-gas automata, Physical Review Letters **61**, 2332 (1988).

[32] D. A. Wolf-Gladrow, *Lattice-gas cellular automata and lattice Boltzmann models: An introduction* (Springer, 2004).

[33] S. Chen and G. D. Doolen, Lattice boltzmann method for fluid flows, Annual Review of Fluid Mechanics **30**, 329 (1998).

[34] Qiskit Development Team, Summary of quantum operations, `https://qiskit.org/documentation/tutorials/circuits/3_summary_of_quantum_operations.html` (2017).

[35] J. Yepez, Quantum lattice-gas model for the diffusion equation, International Journal of Modern Physics C **12**, 1285 (2001).

[36] J. Yepez, Quantum lattice-gas model for the Burgers equation, Journal of Statistical Physics **107**, 203 (2002).

[37] J. A. Scoville, *Type-II Quantum Computing Algorithm for Computational Fluid Dynamics*, Master's thesis, Air Force Institute of Technolgy (2006).

[38] Google Quantum AI, Quantum computer datasheet, `https://quantumai.google/hardware/datasheet/weber.pdf` (2021).

[39] M. A. Nielsen and I. L. Chuang, *Quantum Computation and Quantum Information*, 10th ed. (Cambridge University Press, Cambridge; New York, 2010).

[40] M. Dobšíček, G. Johansson, V. Shumeiko, and G. Wendin, Arbitrary accuracy iterative quantum phase estimation algorithm using a single ancillary qubit: A two-qubit benchmark, Physical Review A **76**, 030306 (2007).

[41] D. Perez-Garcia, F. Verstraete, M. M. Wolf, and J. I. Cirac, Matrix product state representations, arXiv preprint quant-ph/0608197 (2006).

[42] A. J. McCaskey, E. F. Dumitrescu, D. Liakh, M. Chen, W. Feng, and T. S. Humble, Extreme-scale programming model for quantum acceleration within high performance computing, arXiv preprint arXiv:1710.01794 (2017).

[43] V. Gheorghiu, Quantum++: A modern C++ quantum computing library, PLOS ONE **13** (2018).

[44] A. McCaskey, E. Dumitrescu, M. Chen, D. Lyakh, and T. Humble, Validating quantum-classical programming models with tensor network simulations, PLOS ONE **13**, e0206704 (2018).

[45] G. Vidal, Efficient classical simulation of slightly entangled quantum computations, Physical Review Letters **91**, 147902 (2003).

[46] J. Yepez, Quantum computation of fluid dynamics (1998), AFRL, Access No. ADA437298.